Compressible Equilibrium Turbulent Boundary Layers at Nonadiabatic Wall Conditions

Cindy W. Albertson*
NASA Langley Research Center, Hampton, Virginia 23665
and
Robert L. Ash†
Old Dominion University, Norfolk, Virginia 23508

Experimental data have been obtained to define test conditions necessary for a compressible, naturally developing, equilibrium turbulent boundary layer. The model consisted of a flat plate that was tested in the NASA Langley Research Center 8-ft high temperature tunnel. For the present study, the nominal boundary-layer edge Mach numbers were 5.0 and 6.2. The local Reynolds number based on boundary-layer edge conditions and plate length ranged from 8×10^6 to 39×10^6. The nominal ratio of adiabatic wall to actual wall temperature was 5.4, due to both the high total temperature of 3300°R and the heat-sink characteristics of the model. This temperature ratio is considerably higher than that obtained in previous compressible boundary-layer studies and simulates hypersonic flight under highly cooled wall conditions, which are anticipated for hypersonic cruise vehicles. The data indicate that a momentum thickness Reynolds number of at least 4000 is required for an equilibrium turbulent boundary layer, which is in approximate agreement with incompressible studies. This criterion was determined by comparing the transformed wake strength of the boundary layer with the incompressible data of Coles. Also, several shape factors were examined and found to support the trend shown by the wake strength.

Nomenclature

C = intercept for logarithmic law, Eq. (5)
C_f = local skin friction coefficient, $2\tau_w/(\rho_e U_e^2)$
c_p = specific heat at constant pressure, Btu/lb$_m$-°R
G = Clauser's shape factor, Eq. (11)
H = enthalpy, Btu/lb$_m$
h = heat transfer coefficient, Btu/ft^2-s-°R
K = slope for logarithmic law, Eq. (5)
k = thermal conductivity, Btu/ft-s-°R
M = Mach number
N = velocity power law exponent, Eq. (4)
Pr = Prandtl number, $\mu c_p/k$
p = pressure, psia
$\dot{q}$ = heat transfer rate, Btu/ft^2-s
Re_∞ = freestream unit Reynolds number, $\rho_\infty U_\infty/\mu_\infty$, 1/ft
Re_x = local Reynolds number based on boundary-layer edge temperature, $\rho_e U_e x/\mu_e$
Re^* = local unit Reynolds number based on reference temperature, $\rho^* U_e/\mu^*$, 1/ft
Re_x^* = local Reynolds number based on reference temperature, $\rho^* U_e x/\mu^*$
Re_v^* = Reynolds number corresponding to the virtual origin of the turbulent boundary layer, $\rho^* U_e x_v/\mu^*$
Re_θ = momentum thickness Reynolds number based on boundary-layer edge temperature, $\rho_e U_e \theta/\mu_e$
Re_θ^* = momentum thickness Reynolds number based on reference temperature, $\rho^* U_e \theta/\mu^*$
St = Stanton number based on boundary-layer edge temperature, $\dot{q}/(H_{aw} - H_w)\rho_e U_e$
St^* = Stanton number based on reference temperature, $\dot{q}/(H_{aw} - H_w)\rho^* U_e$
T = temperature, °R
U = velocity, ft/s
$\overline{U}$ = transformed velocity, ft/s, Eq. (7)
U_τ = shear velocity, $(\tau_w/\rho_w)^{1/2}$, ft/s
x,y = coordinates for surface instrumentation, ft (see Fig. 2)
z = distance measured normal from plate surface, in.
α = angle of attack, deg
β = pressure gradient parameter, $\delta^*/\tau_w(dp/dx)$
δ = boundary-layer thickness, in.
δ^* = displacement thickness, in., Eq. (8)
δ_H = total enthalpy thickness, in., Eq. (13)
Δ = defect thickness, in., Eq. (12)
Δx_{tr} = surface distance from end of transition to measuring station, in.
γ = ratio of specific heats
θ = momentum thickness, in., Eq. (9)
μ = viscosity, lb$_m$/ft-s
ν = kinematic viscosity, ft^2/s
Π = wake parameter, Eq. (5)
ρ = density, lb$_m$/ft^3
τ_w = skin friction, psi

Subscripts and Superscript

aw = adiabatic wall
e = boundary-layer edge (just outside the boundary layer)
t = total condition
tc = total condition in the combustor
te = total condition at the boundary-layer edge
U = velocity
v = virtual origin of the turbulent boundary layer
w = wall
∞ = freestream
$*$ = condition at Eckert's reference enthalpy, Eq. (1)

Presented as Paper 90-1410 at the AIAA 16th Ground Testing Conference, June 18-20, 1990, Seattle, WA; received July 25, 1990; revision received Dec. 4, 1990; accepted for publication Dec. 6, 1990.

*Aerospace Technologist, Aerothermal Loads Branch, Structural Mechanics Division, Mail Stop 395.
†Professor, Department of Mechanical Engineering and Mechanics. Associate Fellow AIAA.

Introduction

THE design of hypersonic vehicles requires a detailed knowledge of the boundary-layer behavior over the vehicle. Due to the flight regime anticipated for vehicles of current interest, the boundary layer is expected to be turbulent over much of the vehicle and influenced by large differences between the flow-based adiabatic wall temperature and the actual wall temperature. The predictive capabilities needed to provide design information for complex flow regions of these vehicles have been found to be deficient.[1-3] Shock-wave turbulent boundary-layer interactions, which are expected to occur inside the engine inlet as well as on other regions of the vehicle, are one class of flows that are particularly difficult to predict.

Because of the flow complexity, wind tunnel experiments are needed both to obtain the required design information and to provide test data for numerical prediction validations. However, wind tunnel experiments that require turbulent boundary-layer flows ahead of the shock-wave interaction zone are very difficult to design and control. Specifically, if the turbulent boundary layer is not fully developed and approximately two-dimensional, the shock-wave boundary-layer interaction may be unique to the wind tunnel and therefore of limited usefulness. Fully turbulent boundary layers occur after the transition process from laminar to fully turbulent flow is complete. Such boundary layers are considered to be equilibrium turbulent flows, as defined by low-speed researchers.[4,5] Incompressible studies[6-8] have shown that these flows exhibit certain mean and fluctuating characteristics that are nearly independent of Reynolds number. For naturally developing flat plate flows, these incompressible studies have shown that fully developed turbulence occurs at Reynolds numbers based on momentum thickness Re_θ of about 5000 or greater. Compressible studies of such flows have been much less rigorous and have focused primarily on the behavior of the velocity power law exponent.[9,10]

The primary purpose of the present paper is to define appropriate test conditions required to produce a naturally developing, hypersonic, equilibrium turbulent boundary layer. Additionally, the paper presents some new hypersonic turbulent boundary-layer data at higher temperature ratios than previously available. The model consisted of a flat plate that was tested in the NASA Langley Research Center 8-ft high temperature tunnel. This facility simulates true temperature flight conditions at a nominal Mach number of 7. For the present study, the nominal adiabatic wall to actual wall temperature ratio was 5.4, due to both the high total temperature of 3300°R and the heat-sink characteristics of the model. This temperature ratio is considerably higher than that obtained in previous compressible boundary-layer studies[11] and simulates hypersonic flight under highly cooled wall conditions, such as that anticipated for hypersonic cruise vehicles. The model was inclined to the flow to increase the local Reynolds number, producing nominal boundary-layer edge Mach numbers of 5.0 and 6.2. The local Reynolds number, based on boundary-layer edge conditions and model length, ranged from 8×10^6 to 39×10^6.

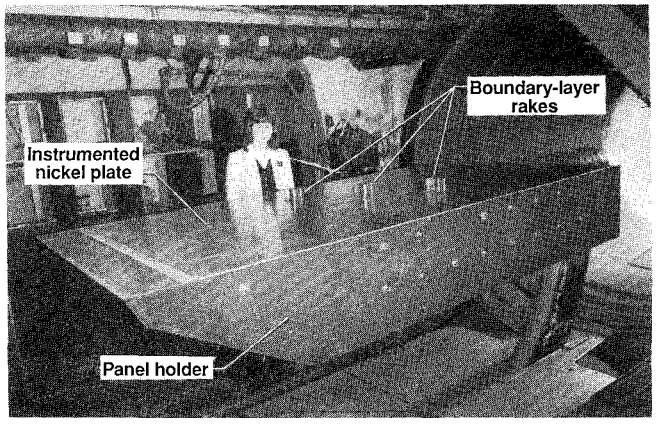

Fig. 1 Panel holder in the NASA Langley 8-ft high temperature tunnel test chamber.

The boundary layer was surveyed at various locations on the plate using pitot pressure, static pressure, and total temperature probes to obtain mean velocity and temperature profiles. In addition, surface pressure distributions were measured to ensure uniform flow conditions. Surface heating rates, inferred from surface temperature measurements, were obtained to determine conditions in which the boundary layer had transitioned from laminar to turbulent flow. The details of these measurements are reported elsewhere.[12]

The compressible boundary layer was assessed using the established time-averaged incompressible descriptions of equilibrium turbulent boundary layers given by Clauser[5] and Coles.[4] To correlate compressible boundary-layer velocity profiles with the incompressible relations, van Driest's transformation[13] was employed. This transformation has been shown previously[11] to provide a reasonably good correlation for temperature ratios up to 3.3. The transformed wake strength of the boundary layer was compared with the data of Coles[6] for incompressible boundary layers. In addition, various shape factors were examined and support the results from the wake strength.

Description of Experiment

Model and Instrumentation

The model used for the present study consisted of a large, instrumented flat plate. The plate was made of Nickel 200 and was mounted on the panel holder, a generalized test apparatus for the NASA Langley Research Center 8-ft high temperature tunnel (8 ft HTT) (see Fig. 1). A sharp copper leading edge was attached to the front of the panel holder. The overall length and width of the model was 9.7 and 4.3 ft, respectively. The plate dimensions and instrumentation layout are shown in Fig. 2. The surface of the plate was hydraulically smooth[12] and instrumented with pressure orifices, coaxial surface thermocouples, and boundary-layer rake assemblies. Pressure measurements were obtained to assess spanwise and longitudinal pressure gradients on the plate and are discussed in detail by Albertson.[12] These measurements indicate that the pressure gradient parameter β, where $\beta = \delta^*/\tau_w(dp/dx)$, varied no more than ± 0.01. Heating rates, inferred from transient surface temperature measurements using a semi-infinite slab technique,[14] were used to assess transition from laminar to turbulent flow. Boundary-layer rake assemblies, consisting of total pressure, static pressure, and total temperature probes (see Fig. 3), were used to survey the boundary layer at various locations on the plate. The pitot pressure and total temperature probes were flattened horizontally to minimize vertical averaging effects and were clustered near the wall. Additional details regarding the model, instrumentation, data reduction, and error analysis are presented elsewhere.[12]

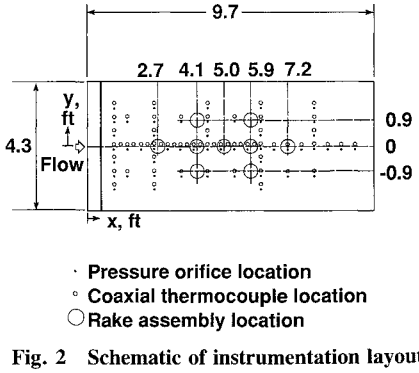

Fig. 2 Schematic of instrumentation layout.

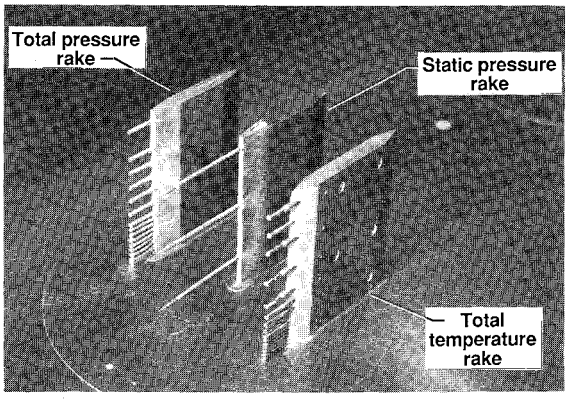

Fig. 3 Boundary-layer rake assembly.

Test Facility

A schematic of the 8 ft HTT is shown in Fig. 4. This facility is a large blowdown wind tunnel that provides true temperature flight simulation at a nominal freestream Mach number of 7 and at pressure altitudes between 80,000 and 120,000 ft. The high energy test medium is obtained by burning a mixture of methane and air under high pressure in a combustor. The combustion products are expanded to the test chamber Mach number by means of a conical-contoured nozzle with an exit diameter of 8 ft. The flow in the test chamber is a free jet that enters a straight tube supersonic diffuser where it is pumped to the atmosphere by means of a single-stage annular air ejector. The tunnel can be operated at total temperatures between 2300°R and 3600°R and freestream dynamic pressures between 240 and 1800 psf. The corresponding freestream Reynolds number, based on a model length of 10 ft, ranges between 3×10^6 and 30×10^6. The maximum run time of the facility is 120 s.

Models are positioned beneath the test chamber during tunnel startup and shutdown to minimize aerodynamic loads. Once flow conditions are established, the model is inserted into the flow using a hydraulically actuated elevator. Before tunnel shutdown, the model is withdrawn from the flow. For the present model, the insertion time required to move the model from the edge of the test core to the tunnel centerline was 1.0 s. The model was exposed to the flow for approximately 4 s. All data were obtained within the first 2 s of exposure. The model wall temperature typically increased from 540°R to 600°R during this 2-s period.

The facility is currently being modified to facilitate testing of hypersonic air-breathing propulsion systems. The modified facility will use oxygen enrichment to raise the oxygen content to match that of air and will have alternate Mach number capabilities of 4 and 5, in addition to the Mach 7 capability. Additional details of the 8 ft HTT can be found in Ref. 15.

Test Conditions

The tests were conducted at a total temperature of approximately 3300°R, which corresponded to a ratio of adiabatic wall to actual wall temperature, T_{aw}/T_w, of 5.4. Additionally, limited data were obtained at a lower total temperature of 2700°R, corresponding to a temperature ratio of 4.4. The nominal freestream Mach number was 7, and the freestream Reynolds number, based on plate length, ranged from 5.5×10^6 to 18×10^6. To increase the local Reynolds number, the model was pitched at angles of attack of 5 and 13 deg, producing boundary-layer edge Mach numbers of approximately 6.2 and 5.0, respectively. The local Reynolds number, based on plate length and boundary-layer edge conditions, ranged from 8×10^6 to 39×10^6. Most of the tests were conducted at an angle of attack of 13 deg. This angle of attack was found to be necessary to increase the local Reynolds number sufficiently to produce large areas of equilibrium turbulent boundary-layer flows over the plate.[12] The

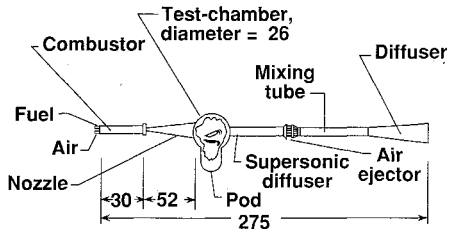

Fig. 4 NASA Langley 8-ft high temperature tunnel (all dimensions in ft).

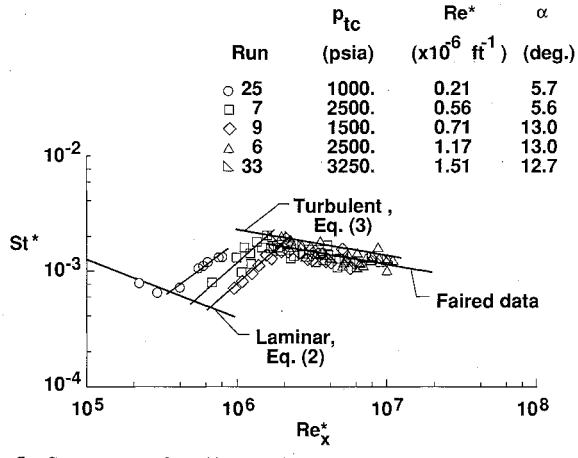

Fig. 5 Stanton number distributions for various test conditions (y = 0.1 ft, T_{aw}/T_w = 5.6).

momentum thickness Reynolds number Re^*_θ, at the probe locations, calculated using an enthalpy-based reference temperature, ranged from 400 to 7800.

Results and Discussion

Surface Heating Distributions

Before surveying the boundary layer, transition from laminar to turbulent flow was first assessed using the heating rate data. The longitudinal heating rate distributions, shown in Fig. 5, are nondimensionalized in terms of Stanton and Reynolds numbers calculated using a local reference temperature. The reference temperature is defined in terms of enthalpy using a correlation given by Eckert[16]:

$$H^* = H_e + 0.50(H_w - H_e) + 0.22(H_{aw} - H_e) \quad (1)$$

The temperature corresponding to the reference enthalpy was obtained from temperature-enthalpy charts for methane-air combustion products given by Leyhe and Howell.[17]

Laminar and turbulent Stanton number predictions[18] are presented with the data to assist in defining conditions at which the boundary layer is turbulent. The laminar prediction is a similarity solution to the energy equation for a laminar boundary layer developing along a flat plate under constant freestream velocity and temperature conditions. This equation is given as

$$St^* = 0.332\, Pr^{*(-2/3)}\, Re_x^{*(-1/2)} \quad (2)$$

The turbulent prediction was derived by solving the momentum integral equation assuming a velocity power law exponent of 7 and employing a Reynolds analogy. This equation is given as[18]

$$St^* = 0.0287\, Pr^{*(-2/5)}\, (Re_x^* - Re_v^*)^{(-1/5)} \quad (3)$$

In Eq. (3), Re^*_v is the Reynolds number corresponding to the virtual origin of the turbulent boundary layer. For the present comparison, this quantity was determined by first

correlating the local Reynolds number Re_x^* with the momentum thickness Reynolds number Re_θ^*, using a least squares curve fit.[12] Then Re_v^* was determined to be 1.27×10^6 by extrapolating this correlation to an Re_θ^* of zero.

In Fig. 5, the heat transfer data are shown for various test conditions. The Reynolds number corresponding to the start of transition increases with increasing unit Reynolds number, a trend that has been shown by other data obtained in the 8 ft HTT[19] as well as data obtained in flight and in other facilities.[20] This trend has been the subject of much debate but currently has no explanation. The heat transfer data also indicate fully turbulent heating levels for Reynolds numbers Re_x^* of 2×10^6 and greater. However, this may not indicate a fully turbulent boundary layer since incompressible boundary-layer studies[7] have shown that fully turbulent wall region behavior occurs almost immediately after the start of transition. The outer wake of the boundary layer is the last region to reach equilibrium after transition. Therefore, the Reynolds number required for an equilibrium turbulent boundary layer should be higher than that indicated by surface heating rates. Boundary-layer profiles, particularly of the wake region, have been studied in some detail and are discussed in the following sections to assess conditions for equilibrium turbulent flow.

Boundary-Layer Velocity Profiles

Typical velocity distributions for various locations on the plate are shown in Fig. 6 for Reynolds numbers Re_x^* ranging from 5.0×10^6 to 8.3×10^6. The local velocities are normalized with respect to the boundary-layer edge velocity U_e and are plotted as a function of their location in the velocity boundary layer z/δ_U. The velocity distributions show an inflection near the wall that can be attributed to pitot probe interference, as discussed in Ref. 12. With this qualification, the profiles appear to be self-similar at these Reynolds numbers.

To compare with previous compressible boundary-layer data, the velocity distributions from the present study are plotted in terms of the velocity power law exponent N in Fig. 7 where N is defined by the following relationship:

$$\frac{U}{U_e} = \left(\frac{z}{\delta_U}\right)^{\frac{1}{N}} \tag{4}$$

The velocity power law exponent is plotted as a function of momentum thickness Reynolds number based on boundary-layer edge conditions Re_θ. Here Re_θ was chosen to compare the present data, obtained at temperature ratios T_{aw}/T_w ranging from 4.4 to 5.4, with compressible data[9,10] obtained at temperature ratios ranging from 1.5 to 3.3, as represented by the shaded region. Fenter's[21] empirical curve for subsonic and supersonic data obtained at adiabatic wall conditions is also shown for comparison purposes. A parallel scale for Re_x^* (applicable for $T_{aw}/T_w = 5.4$) is shown to relate the power law exponents to the heating data shown in Fig. 5. The three data points from the present study near $Re_\theta = 2 \times 10^3$ correspond to an Re_x^* near 1×10^6 and are known to be in the transitional boundary-layer region according to the heating data in Fig. 5. These three points are contained within the "overshoot" region of the data of Refs. 9 and 10. Johnson and Bushnell[10] showed that this overshoot phenomenon is related to transition and correlated the end of overshoot with the ratio of the distance from the end of transition Δx_{tr} (as indicated by the heating-rate data) to the boundary-layer thickness δ at the profile location. As indicated in Fig. 7, overshoot is not present in the data for $\Delta x_{tr}/\delta \geq 30$, a result that is consistent with that of Johnson and Bushnell. Hopkins et al.[9] observed that the overshoot behavior in their data for Re_θ below 6×10^3 was absent from their finite-difference calculations for equilibrium flow conditions and attributed this behavior to nonequilibrium flow. For Re_θ above 6×10^3 (or Re_x^* above 3×10^6), the exponents show a slight logarithmic increase with Re_θ, as indicated by the data of Refs. 9 and 10 and by the curve fit equation for adiabatic walls.[21] Overall, the exponents from the present investigation show trends and levels that are consistent with earlier work and support the contention that equilibrium turbulent boundary-layer flow can be obtained for Re_x^* above 3×10^6. As anticipated, this is higher than the value of 2×10^6 indicated by the heating rate data. However, further comparisons were deemed necessary before any final conclusions could be drawn.

Comparison with Coles' Incompressible Data

For turbulent boundary layers, Coles[4] proposed that for smooth walls, the velocity profile outside the laminar sublayer can be described by the following incompressible law of the wall correlation:

$$\frac{U}{U_\tau} = \frac{1}{K} \ln\left(\frac{zU_\tau}{\nu}\right) + C + \frac{2\Pi}{K} \sin^2\left(\frac{\pi}{2}\frac{z}{\delta_U}\right) \tag{5}$$

In Eq. (5), the wake parameter Π is given as $\Pi = 0.8(\beta + 0.5)^{0.75}$ where $\beta = (\delta^*/\tau_w)(dp/dx)$ (Ref. 22). Also, the constants K and C are given as 0.41 and 5.0, respectively.[4] Equation (5) can be expressed, alternatively, in terms of the velocity defect relation:

$$\frac{U_e - U}{U_\tau} = \frac{-1}{K} \ln\frac{z}{\delta_U} + \frac{\Pi}{K}\left[2 - \sin^2\left(\frac{\pi}{2}\frac{z}{\delta_U}\right)\right] \tag{6}$$

Equation (6) has been shown by Clauser[5] to represent a universal velocity profile that is independent of distance (or Reynolds number), provided that the wake parameter Π is a constant.

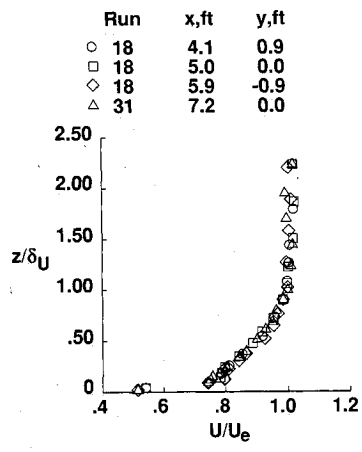

Fig. 6 Typical velocity distributions for various locations on the plate ($5.0 \times 10^6 \leq Re_x^* \leq 8.3 \times 10^6$, $M_e = 5.0$, $T_{aw}/T_w = 5.3$).

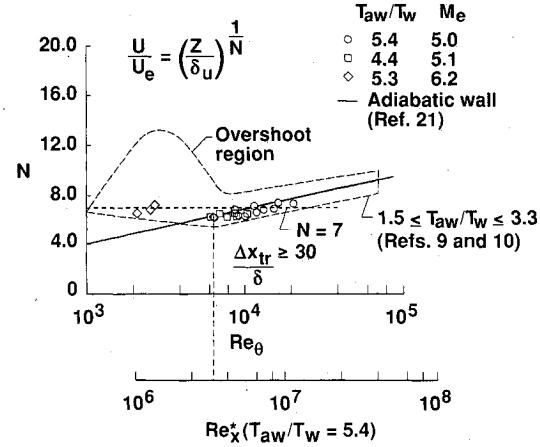

Fig. 7 Power law exponent variation with Reynolds number.

Although these correlations were developed from incompressible experiments, Fernholz and Finley[11] suggested that they are applicable to compressible flows provided that the density variation through the boundary layer is taken into account. They showed that the compressible transformation derived by van Driest[13] provides a reasonably good correlation between compressible data and the incompressible correlations of Coles [Eqs. (5) and (6)]. Van Driest's transformation is given as

$$\bar{U} = \frac{U_e}{a}\left\{\sin^{-1}\left[\frac{(2a^2U/U_e) - b}{Q}\right] + \sin^{-1}\frac{b}{Q}\right\} \quad (7)$$

where

$$a = \left(\frac{\gamma - 1}{2} M_e^2 \frac{T_e}{T_{aw}}\right)^{1/2}, \qquad b = \left(\frac{T_{aw}}{T_w} - 1\right)$$

$$Q = (b^2 + 4a^2)^{1/2}$$

A typical semilogarithmic plot of a velocity distribution that has been transformed using Eq. (7) and plotted in wall coordinates is shown in Fig. 8 with the various regions of the boundary layer delineated. Because skin friction measurements were unavailable, the profile was adjusted to fit the logarithmic portion of Eq. (5). Also indicated in Fig. 8 is the wake strength of the boundary layer $\Delta\bar{U}/U_\tau$. The wake strength is defined as the maximum velocity increase in the wake region of the boundary layer above the logarithmic equation shown on the plot. This wake strength is related to the wake parameter Π such that $\Delta\bar{U}/U_\tau = 2\Pi/K$. Because K is a constant, the wake strength is also a constant for equilibrium flow. In Ref. 6, Coles has shown that for incompressible flow, this wake strength approaches a constant of approximately 2.7 with increasing momentum thickness Reynolds number.

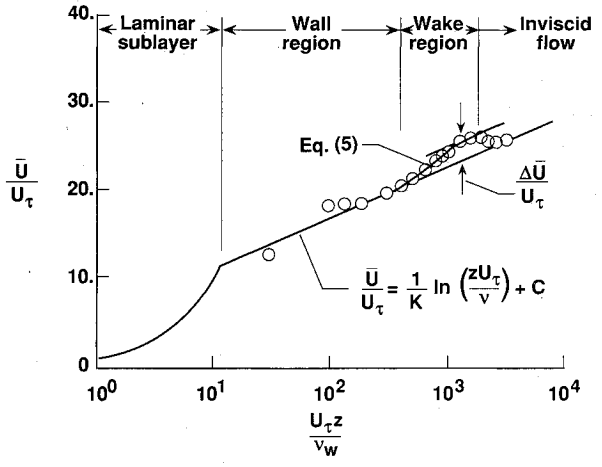

Fig. 8 Typical velocity distribution in wall coordinates ($Re_x^* = 8.3 \times 10^6$, $M_e = 5.0$, $T_{aw}/T_w = 5.3$).

The wake strengths from the present investigation are compared with the incompressible compilation of Coles[6] in Fig. 9. For the present data, the momentum thickness Reynolds number is evaluated at a reference temperature, corresponding to Eckert's[16] reference enthalpy [Eq. (1)], rather than at the boundary-layer edge temperature because this gives the best agreement with the trends of the incompressible data. The present data show similar trends to that of Coles but are generally low. The data indicate equilibrium turbulent boundary-layer behavior at an Re_θ^* of approximately 4000 and above. This corresponds to a local Reynolds number Re_x^* of nearly 6×10^6 for a nominal temperature ratio of 5.4. This is approximately twice the value of Re_x^* indicated by the power law exponents in Fig. 7 and three times the Reynolds number corresponding to the end of transition inferred from the heat transfer data in Fig. 5. Because of low resolution in the wall region (see Fig. 8), the present wake strengths may have limited accuracy. Consequently, various shape factors were examined and are discussed in the next section.

Shape Factors

To obtain the shape factors presented in this section, the velocity and density distributions, inferred from the pressure and temperature measurements, were integrated over the thickness of the boundary layer. The velocities affected by probe interference were corrected using the appropriate power law variation before integrating the distributions.

Initially, the shape factor δ^*/θ was examined where the displacement thicknesses δ^* and momentum thicknesses θ were calculated from the boundary-layer rake measurements using

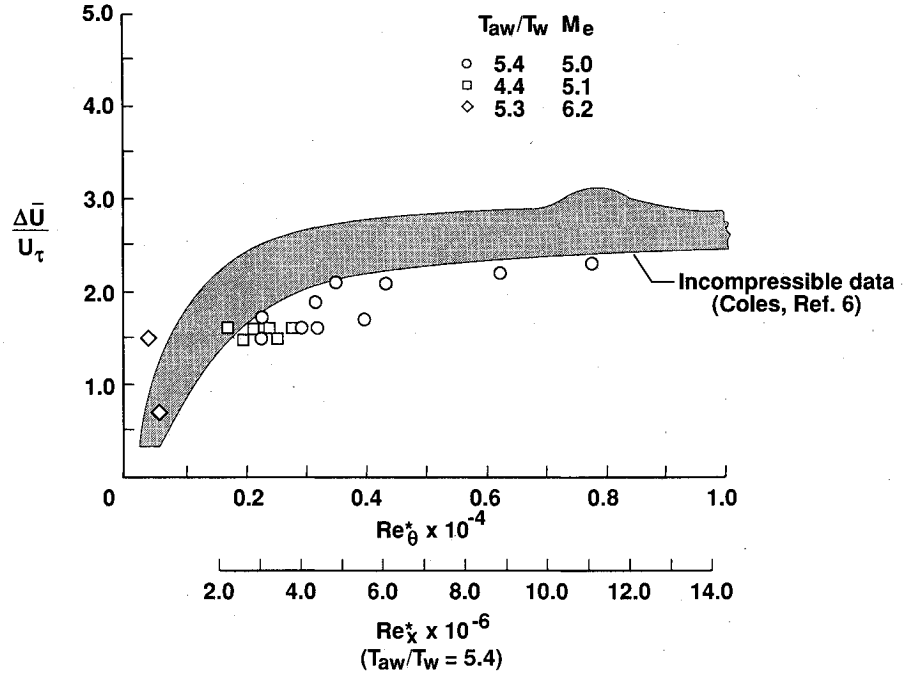

Fig. 9 Variation of wake strength $\Delta\bar{U}/U_\tau$ with Reynolds number.

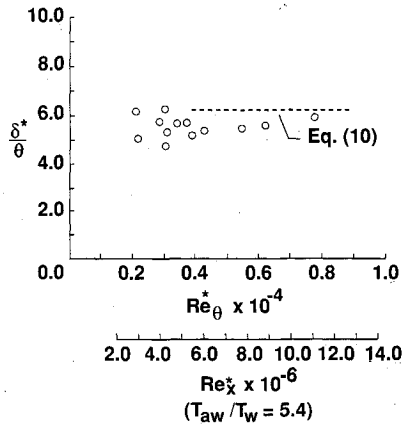

Fig. 10 Variation of shape factor δ^*/θ with Reynolds number (M_e = 5.0, T_{aw}/T_w = 5.4).

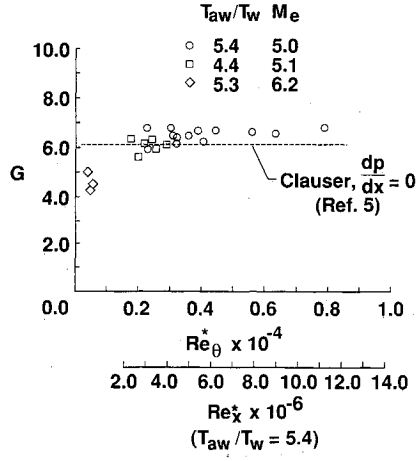

Fig. 11 Variation of Clauser's shape factor G with Reynolds number.

the standard definitions for compressible flow[23]:

$$\delta^* = \int_0^\infty \left(1 - \frac{\rho U}{\rho_e U_e}\right) dz \tag{8}$$

$$\theta = \int_0^\infty \frac{\rho U}{\rho_e U_e}\left(1 - \frac{U}{U_e}\right) dz \tag{9}$$

The shape factor δ^*/θ is plotted as a function of Re_θ^* in Fig. 10. Also shown with the data is the empirical correlation of δ^*/θ with Mach number, power law exponent, and temperature ratio given by Hopkins et al.[9]:

$$\frac{\delta^*}{\theta} = \frac{(N+2)(1+0.344\,M_e^2)}{N\,[2-(T_w/T_{aw})]^{1.17}} \tag{10}$$

The data show some scatter for values of Re_θ^* below approximately 4000 and then a slight linear increase for values of Re_θ^* above 4000. This behavior is consistent with that of the wake strength (Fig. 9) that also showed some scatter below $Re_\theta^* = 4000$. However, the wake strength approached a constant near $Re_\theta^* = 4000$, indicating that it is independent of Reynolds number above this value. The data are generally below Hopkins' correlation, Eq. (10), which was derived from data obtained at lower wall temperature ratios (ranging from adiabatic, or 1.0, to 3.3).

In an attempt to find a shape factor that is less sensitive to Reynolds number for classifying turbulent boundary layers, Clauser[5] derived a shape factor G based on the area beneath the velocity defect curve given by Eq. (6). The equation for G is given as

$$G = \frac{1}{\Delta}\int_0^\infty \left(\frac{U-U_e}{U_\tau}\right)^2 dz \tag{11}$$

where

$$\Delta = \int_0^\infty \left(\frac{U_e - U}{U_\tau}\right) dz \tag{12}$$

Clauser determined from his incompressible data that for a zero pressure gradient equilibrium turbulent boundary layer, $G = 6.1$. This shape factor has been examined for the present study to compare with the results indicated by the shape factor δ^*/θ, wake strength $\Delta\overline{U}/U_\tau$, power law exponent N, and the heating data. In Fig. 11, the shape factors G, evaluated using transformed velocities [Eq. (7)], are shown along with Clauser's incompressible value of $G = 6.1$. Below an Re_θ^* of 4000, the data show a general downward trend, similar to the trend shown by the wake strength in Fig. 9. Above an Re_θ^* of 4000, the data are approximately equal to a constant value of 6.8, which is reasonably close to Clauser's incompressible value.

Because a thermal boundary layer also exists for the present study, the thermal shape factor δ_H/θ was examined for uniformity. The quantity δ_H represents the total enthalpy thickness that is defined as[23]

$$\delta_H = \int_0^\infty \frac{\rho U}{\rho_e U_e}\left(\frac{H_{te} - H_t}{H_{te} - H_w}\right) dz \tag{13}$$

The shape factor δ_H/θ is based on the integral form of the momentum and energy equations, assuming a two-dimensional, zero pressure gradient boundary layer. These integral equations are given as[18]

Momentum:

$$\frac{d\theta}{dx} = \frac{C_f}{2} \tag{14}$$

Energy:

$$\frac{d\delta_H}{dx} = St \tag{15}$$

These equations can be related using the turbulent Reynolds analogy[18]

$$C_f = 2\,St\,Pr^{(2/5)} \tag{16}$$

Substituting Eqs. (14) and (15) into Eq. (16) and rearranging yields

$$\frac{d\delta_H}{d\theta} = \frac{1}{Pr^{(2/5)}} \tag{17}$$

Integrating Eq. (17) yields

$$\frac{\delta_H}{\theta} = \frac{1}{Pr^{(2/5)}} + \frac{B}{\theta} \tag{18}$$

In Eq. (18), B is a constant that can be determined experimentally.

In Fig. 12, the thermal shape factor δ_H/θ is shown as a function of Re_θ^*. Note that the data approach a constant close to $1/Pr^{(2/5)}$ above $Re_\theta^* = 4000$. (For the present methane-air combustion products test medium, $1/Pr^{(2/5)} = 1.12$.) This implies that the constant B in Eq. (18) is zero. However, additional data above $Re_\theta^* = 4000$ are needed to support this contention.

In general, the shape factors δ^*/θ, G, and δ_H/θ (see Figs. 10–12) all support the results of the wake strength in Fig. 9 and indicate equilibrium turbulent flow can be assumed for Re_θ^* above 4000. This result is in approximate agreement with

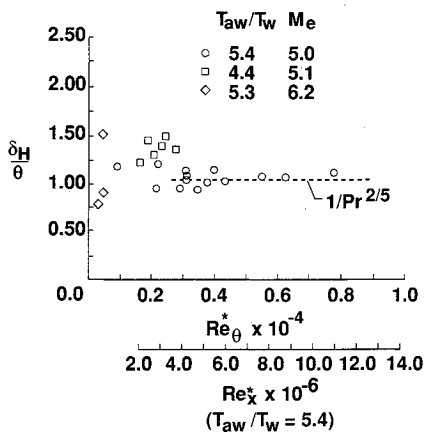

Fig. 12 Variation of thermal shape factor δ_H/θ with Reynolds number.

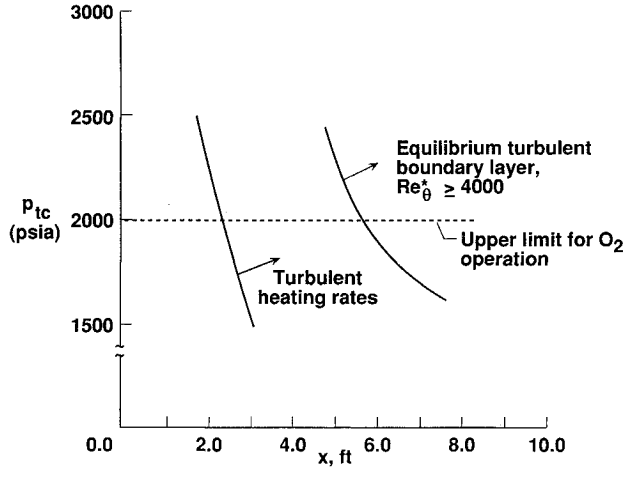

Fig. 13 Test conditions for a flat plate equilibrium turbulent boundary layer in the NASA Langley 8-ft high temperature tunnel (Mach 7 nozzle, T_{tc} = 3300°R, α = 13 deg).

incompressible studies. For a nominal temperature ratio of 5.4, this value of Re_θ^* corresponds to a local Reynolds number Re_x^* of nearly 6×10^6. As mentioned previously, this is approximately twice the value indicated by the power law exponents in Fig. 7 and three times the Reynolds number corresponding to the end of transition from the heat transfer data shown in Fig. 5.

Test Conditions for an Equilibrium Turbulent Boundary Layer

Based on the above conclusions, the test conditions required for an equilibrium turbulent boundary layer in the 8-ft high temperature tunnel can be expressed in terms of the basic facility operating conditions. In Fig. 13, a test envelope plotted in terms of the minimum combustor total pressure p_{tc} required for equilibrium turbulent flow conditions at various wetted distances x is shown. For comparison purposes, a curve corresponding to the minimum conditions required for turbulent heating levels is also shown. The data correlations are shown for a nominal model angle of attack of 13 deg and a total temperature in the combustor of 3300°R. These conditions correspond to a boundary-layer edge Mach number M_e of 5.0 and a temperature ratio T_{aw}/T_w of 5.4 for a nominal wall temperature of 600°R. The data indicate that at a total pressure of 2000 psia, a wetted distance of at least 5.6 ft is required for equilibrium turbulent flat plate flow. This is significantly higher than the distance of approximately 2.2 ft required for turbulent heating levels and indicates that a relatively large distance is required before turbulent behavior is displayed throughout the boundary layer. This 2000 psia level is significant because it corresponds to the pressure design limit of the oxygen run tank and will therefore be the upper limit for operating with oxygen enrichment, once the ongoing facility modification is complete.[15] When the facility is operated without oxygen enrichment, this oxygen tank will be isolated. The facility can then be operated up to 4000 psia, which is the pressure design limit of the combustor.

Conclusions

Experimental data have been obtained to define test conditions necessary to establish a compressible, naturally developing, equilibrium turbulent boundary layer. The model consisted of a flat plate that was tested in the NASA Langley Research Center 8-ft high temperature tunnel. For the present study, the nominal boundary-layer edge Mach numbers were 5.0 and 6.2. The ratio of adiabatic wall to actual wall temperature was 5.4, due to a combination of a high total temperature of 3300°R and the heat-sink characteristics of the model. This temperature ratio was considerably higher than that obtained in previous compressible boundary-layer studies[11] and simulates hypersonic flight under highly cooled wall conditions, which are anticipated for hypersonic cruise vehicles. The momentum thickness Reynolds number Re_θ^*, calculated using an enthalpy-based reference temperature, ranged from 400 to 7800. This corresponded to a local Reynolds number Re_x^* that ranged from 0.7×10^6 to 11×10^6.

The data showed that a momentum thickness Reynolds number of at least 4000 is required for an equilibrium turbulent boundary layer, which is in approximate agreement with incompressible studies. This criteria was determined by comparing the transformed wake strength of the boundary layer with the data of Coles[6] for incompressible boundary layers. Also, several shape factors were examined and supported the results from the wake strength. For the present test conditions, this value of momentum thickness Reynolds number corresponds to an Re_x^* of nearly 6×10^6, which is approximately twice the value indicated by the velocity power law exponents derived from the velocity data and three times the Reynolds number corresponding to the end of transition from the heating rate data.

Based on the above results, a test envelope was developed that defines equilibrium turbulent boundary-layer flow conditions for the 8-ft high temperature tunnel in terms of the basic facility operating conditions. The operating envelope was defined for the Mach 7 nozzle configuration.

References

[1]Holden, M. S., "A Review of Aerothermal Problems Associated with Hypersonic Flight," AIAA Paper 86-0267, Jan. 1986.

[2]Graves, R., Jr., and Hunt, J. L., "NASA's Hypersonic Fluid and Thermal Physics Programs," AIAA Paper 85-0922, June 1985.

[3]Settles, G. S., and Dolling, D. S., "Swept Shock Wave/Boundary-Layer Interactions," *Tactical Missle Aerodynamics*, edited by M. J. Hemsch and J. N. Nielsen, Progress in Astronautics and Aeronautics, Vol. 104, AIAA, New York, 1986, pp. 297-379.

[4]Coles, D. E., "The Law of the Wake in the Turbulent Boundary Layer," *Journal of Fluid Mechanics*, Vol. 1, Pt. 2, July 1956, pp. 191-226.

[5]Clauser, F. H., "Turbulent Boundary Layers in Adverse Pressure Gradients," *Journal of the Aeronautical Sciences*, Vol. 21, No. 2, 1954, pp. 91-108.

[6]Coles, D. E., "The Turbulent Boundary Layer in a Compressible Fluid," Rand Corp., Rept. R-403-PR, Santa Monica, CA, Sept. 1962.

[7]Smits, A. J., Matheson, N., and Joubert, P. N., "Low Reynolds Number Turbulent Boundary Layers in Zero and Favourable Pressure Gradients," *Journal of Ship Research*, Vol. 27, No. 3, 1983, pp. 147-157.

[8]Erm, L. P., Smits, A. J., and Joubert, P. N., "Low Reynolds Number Turbulent Boundary Layers on a Smooth Flat Surface in a Zero Pressure Gradient," *Turbulent Shear Flows 5*, Springer-Verlag, Berlin and Heidelberg, Germany, 1987, pp. 186-197.

[9]Hopkins, E. J., Keener, E. R., Polek, T. E., and Dwyer, H. A.,

"Hypersonic Turbulent Skin-Friction and Boundary-Layer Profiles on Nonadiabatic Flat Plates," *AIAA Journal*, Vol. 10, No. 1, 1972, pp. 40–48.

[10]Johnson, C. B., and Bushnell, D. M., "Power-Law Velocity-Profile-Exponent Variations with Reynolds Number, Wall Cooling, and Mach Number in a Turbulent Boundary Layer," NASA TN D-5753, April 1970.

[11]Fernholz, H. H., and Finley, P. J., "A Critical Commentary on Mean Flow Data for Two-Dimensional Compressible Turbulent Boundary Layers," AGARD-AG-253, May 1980.

[12]Albertson, C. W., "Evaluation of Equilibrium Turbulence for a Hypersonic Boundary Layer at Nonadiabatic Wall Conditions," M.S. Thesis, Old Dominion Univ., Norfolk, VA, July 1989 (also available as NASA TM-101663, Nov. 1989).

[13]van Driest, E. R., "Turbulent Boundary Layer in Compressible Fluids," *Journal of the Aeronautical Sciences*," Vol. 18, No. 5, 1951, pp. 145–160.

[14]Dunn, M. G., Rae, W. J., and Holt, J. L., "Measurement and Analysis of Heat Flux Data in a Turbine Stage: Part I—Description of Experimental Apparatus and Data Analysis," *Journal of Engineering for Gas Turbines and Power*, Vol. 106, Jan. 1984, pp. 229–233.

[15]Reubush, D. E., Puster, R. L., and Kelly, H. N., "Modification to the Langley 8-Foot High Temperature Tunnel for Hypersonic Propulsion Testing," AIAA Paper 87-1887, July 1987.

[16]Eckert, E. R. G., "Engineering Relations for Heat Transfer and Friction in High-Velocity Laminar and Turbulent Boundary-Layer Flow Over Surfaces With Constant Pressure and Temperature," *Transactions of the ASME*, Vol. 78, No. 6, Aug. 1956, pp. 1273–1283.

[17]Leyhe, E. W., and Howell, R. R., "Thermodynamic, Transport, and Flow Properties of the Combustion Products of a Hydrocarbon Fuel Mixture Burned in Air with Results for Ethylene-Air and Methane-Air Mixtures," NASA TN D-914, Jan. 1962.

[18]Kays, W. M., and Crawford, M. E., *Convective Heat and Mass Transfer*, McGraw-Hill, New York, 1980, pp. 138, 213.

[19]Deveikis, W. D., and Hunt, L. R., "Loading and Heating of a Large Flat Plate at Mach 7 in the Langley 8-Ft High Temperature Structures Tunnel," NASA TN D-7275, Sept. 1971.

[20]Stetson, K. F., "On Predicting Hypersonic Boundary Layer Transition," Air Force Wright Aeronautical Lab, Wright-Patterson AFB, OH, AFWAL-TM-84-160-FIMG, March 1987.

[21]Fenter, F. W., "A New Analytical Method for the Prediction of Turbulent Boundary Layer Characteristics on a Thermally-Insulated Flat Plate at Supersonic Speeds," Defense Research Lab, Univ. of Texas, Austin, TX, Report DRL-343, CF-2095, June 1954.

[22]White, F. M., *Viscous Fluid Flow*, McGraw-Hill, New York, 1974, pp. 480–481.

[23]Schlichting, H., *Boundary Layer Theory*, 7th ed., McGraw-Hill, New York, 1979, pp. 354, 659–660, 680.